Modeling DF/HF CW Lasers: An Examination of Key Assumptions

S. W. Zelazny,* R. J. Driscoll,† J. W. Raymonda,‡ J. A. Blauer,§ and W. C. Solomon¶
Bell Aerospace Textron, Buffalo, N.Y.

The sensitivity of laser performance predictions to the approach used to define critical input parameters is examined. These include: 1) entrance conditions to cavity, i.e., composition, temperature, Mach number, pressures, and their distribution across the boundary layers, 2) effective pressure distribution through the laser cavity, 3) mirror reflectivities, 4) mixing mechanisms of the reacting streams, and 5) chemical kinetics. Two computer codes are used in tandem to compute the laser performance, starting with combustor condition, and computing nozzle heat loss and boundary-layer profiles at the cavity inlet. Closed cavity powers are computed under the assumptions of rotational equilibrium and steady gain-equal-loss in a Fabry-Perot resonator. The kinetic model of Cohen is used to calculate the cavity chemistry. Computed results are found to be very sensitive to the boundary-layer profiles, mixing rates, and cavity pressure distributions. Certain reaction rates, to which the predicted performance is quite sensitive, are also identified.

Nomenclature

A	= area
C_i	= mass fraction of specie i
C_p	= specific heat
CL-II,CL-V,CL-XIV	= names given to laser nozzles described in Refs. 25 and 27-29
D_i	= gross diffusion rate for specie i into a multi component stream
D_{ij}	= binary diffusion coefficient for species i, j
F_w/F_c	= ratio of fluorine atom mass fraction at the wall to the core value
h_i	= static enthalpy of specie i
H	= stagnation enthalpy
H_{cc}	= distance from nozzle centerline to centerline
H_{ec}	= combustor (primary) nozzle exit half height
H_{es}	= lasant (secondary) nozzle exit half height
j_m	= 0 two-dimensional; = 1 axisymmetric flow rate
M_m, M_u, M_E, M_{n_i}	= mixing source terms (Sec. 2)
n_i	= mole/mass ratio of specie i
$\dot{N}_i$	= molar flow rate of specie i
$(\dot{N}_{F_2})_{av}$	$= \dot{N}_F/2 + \dot{N}_{F_2}$
p	= static pressure
P	= closed cavity laser power
r_0, r_L	= mirror reflectivities
R_L	$= \dot{N}_{D_2}$ (or $\dot{N}_{H_2}$)$/(\dot{N}_{F_2})_{av}$
R_3	= gas constant
T	= static temperature
v	= vibrational quantum number
V	= velocity in laser cavity mixed region
x	= distance downstream
α	$= \dot{N}_F/(\dot{N}_{F_2})_{av}$ level of dissociation
η	$= P/(\dot{m}_{F_2})_{av}$ specific efficiency
σ	$= P/\dot{m}_3$, specific power
ψ_c	$= (\Sigma \dot{N}_i)_p/(\dot{N}_{F_2})_{av}$, sum over all species in combustor except final F_2
ψ_{DF}	$= \dot{N}_{DF}/(\dot{N}_{F_2})_{av}$
ψ_L	$= \dot{N}_D/(\dot{N}_{F_2})_{av}$, $\dot{N}_D$ is diluent in secondary
Ω	$= \psi_c + \psi_L + R_L - 2$
Subscripts	
CO	= at lasing cutoff
exp	= experimental value
p	= value in primary nozzle
s	= value in secondary nozzle
th	= theoretical value
3	= value of mixed flow at nozzle exit plane

Note: Barred (¯) represent value in the mixed region (Sec. 2) or a value normalized by its baseline value (Tables 8 and 9).

Presented as Paper 77-63 at the AIAA 15th Aerospace Sciences Meeting, Los Angeles, Calif., Jan. 24-26, 1977; submitted Feb. 18, 1977; revision received Dec. 27, 1977.

Index categories: Lasers; Reactive Flows.

*Staff Scientist, High Energy Laser Technology. Member AIAA.
†Principal Scientist, High Energy Laser Technology. Member AIAA.
‡Research Scientist, High Energy Laser Technology.
§Principal Scientist, High Energy Laser Technology.
¶Director, High Energy Laser Technology.

I. Introduction

The Problem

CHEMICAL lasers are characterized by physical processes covering a broad range of technical disciplines. Analysis and design of these systems requires combining knowledge in areas involving gasdynamics, viscous flow, transitional and turbulent flow, chemical kinetics, radiative phenomena, and numerical analysis. A schematic of the various components of a chemical laser is shown in Fig. 1 and the schematics of two types of nozzle arrays (slit and axisymmetric) are shown in Fig. 2. The goal of the laser designer is to achieve a given laser power output and efficiency through a specification of and/or control of parameters, such as nozzle and flow conditions. Selection of the optimum geometry and operating ranges requires guidance from analyses which accurately characterize the dominant physical processes governing laser performance.

Background

In the last seven years, a number of techniques have been developed which compute laser performance (power) in lasers.[1-16] These methods range in scope from simple algebraic expansions used to establish characteristic mixing and reaction scales[1] to complex multidimensional reacting flow computer analyses.[11-14] The multidimensional analyses allow one to include the often important influences of flow

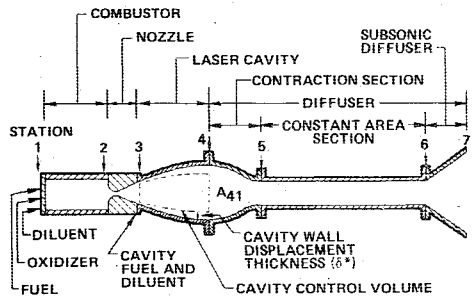

Fig. 1 Schematic of chemical laser components.

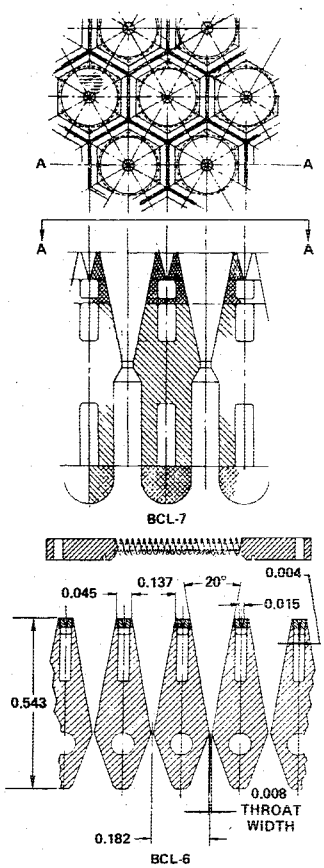

Fig. 2 Schematics of the BCL-6 and BCL-7 nozzles.

striations at the laser cavity entrance induced by the laser nozzle. Unfortunately, this type of two-dimensional mixing and reacting flow analysis does not come cheaply in terms of computer and data preparation time. This fact has resulted in a number of investigators employing one-dimensional idealizations of the flowfield and simulating the mixing using a scheduled mixing model.[8] These resulting analyses still retain the capability of dealing with general chemical systems; however, the effects of boundary-layer influences are not considered.

A compromise between the one- and two-dimensional treatments of the lasing problem can be made by simplifying the multidimensional equations using boundary-layer integral methods. This approach, which allows the nozzle boundary-layer influence to be considered, was used to develop the equation system solved in the BLAZE-II computer code.[16]

It is clear that there are numerous models available to aid in estimating laser performance. These models, depending on their degree of sophistication, require one or more of the following inputs before the zero power gain and/or closed cavity power may be computed: 1) definition of entrance conditions to the laser cavity, i.e., composition, temperature, Mach number, pressures, and spatial distribution of these parameters across the boundary layers which exit each laser

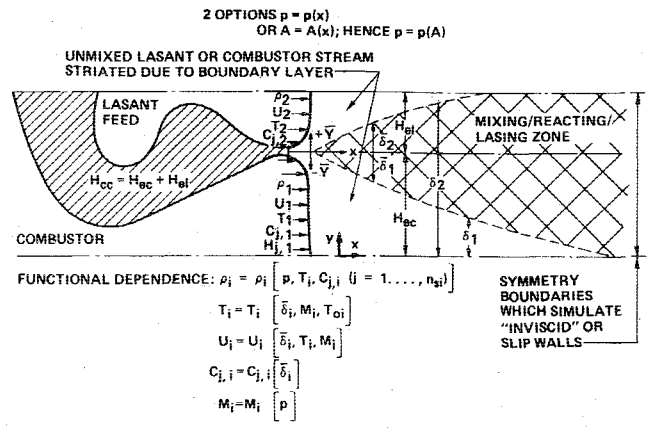

Fig. 3 BLAZE-II flow model and functional dependence of unmixed stream parameters.

nozzle, 2) the effective pressure distribution through the laser cavity, 3) mirror reflectivities, 4) mixing rate of the D_2/H_2 and F streams (laminar, transitional, turbulent, or defined explicitly in terms of mass addition rates), and 5) chemical kinetics (key species, reactions, and reaction rates).

Objective

The objective of this investigation was to establish the sensitivity of laser performance predictions to the approach used in defining each of the preceding parameters. The quasi-two-dimensional form of the BLAZE-II equation system is given in Sec. II, and the chemical rate models are described in Sec. III. The approach used to establish laser cavity inlet conditions is described in Sec. IV. Comparisons between predicted and experimental laser performance are shown in Sec. V for both HF and DF lasers. The sensitivity study is reported in Sec. VI, followed by concluding remarks.

II. Governing Equations

The two-dimensional (x,y) form of the conservation equations is used as the starting point from which a system of governing equations is developed[16] which contains only one independent variable, the main flow direction x. Reduction from two to one independent variable is achieved by integrating the two-dimensional equations across the mixing zone, Fig. 3. It should be noted that the often referred to scheduled mixing analysis[17,18] used in one-dimensional laser flow models will result as a special case of the one-dimensional ordinary differential equation system used herein.

The flow is considered to be either two-dimensional or axisymmetrix and the boundary-layer approximations are assumed to apply. With these assumptions, the governing equations of laminar, transitional, or turbulent flow in terms of their mean (time-averaged) properties can be reduced[16,17] to the following quasi-two-dimensional form.

Continuity:

$$\frac{\mathrm{d}}{\mathrm{d}x}(\rho A V) = M_m \tag{1a}$$

where

$$M_m = 2\pi^j \left(\rho_2 u_2 \delta_2^j \frac{\mathrm{d}\delta_2}{\mathrm{d}x} - \rho_2 v_2 \delta_2^j - \rho_1 u_1 \delta_1^j \frac{\mathrm{d}\delta_1}{\mathrm{d}x} + \rho_1 v_1 \delta_1^j\right) \tag{1b}$$

Momentum:

$$\bar{V}\frac{\mathrm{d}\bar{V}}{\mathrm{d}x} = -\frac{1}{\bar{\rho}}\frac{\mathrm{d}p}{\mathrm{d}x} + M_u \tag{2a}$$

where

$$M_u = \frac{2\pi^j}{\bar{\rho}\bar{A}}\left(\rho_2 u_2^2 \delta_2^j \frac{d\delta_2}{dx} - \rho_2 u_2 v_2 \delta_2^j - \rho_1 u_1^2 \delta_1^j \frac{d\delta_1}{dx} + \rho_1 u_1 v_1 \delta_1^j\right)$$

$$+ \frac{2\pi^j}{\bar{\rho}\bar{A}}(\tau_{m,2}\delta_2^j - \tau_{m,1}\delta_1^j) - \frac{\bar{V}M_m}{\bar{\rho}\bar{A}} \tag{2b}$$

Species continuity:

$$\frac{d\bar{c}_i}{dx} = \frac{1}{\rho V}\bar{\omega}_{i,ch} + M_{c_i} \tag{3a}$$

where

$$M_{c_i} = \frac{2\pi^j}{\dot{m}}\left(\rho_2 u_2 c_{i,2}\delta_2^j \frac{d\delta_2}{dx} - \rho_2 v_2 c_{i,2}\delta_2^j - \rho_1 u_1 c_{i,1}\delta_1^j \frac{d\delta_1}{dx}\right.$$

$$\left. + \rho_1 v_1 c_{i,1}\delta_1^j\right) + \tau_{c,2}\delta_2^j - \tau_{c,1}\delta_1^j - \frac{c_i}{\dot{m}}M_m \tag{3b}$$

Energy:

$$\frac{\bar{c}_p}{T}\frac{d\bar{T}}{dx} - \frac{1}{\bar{\rho}\bar{T}}\frac{d\bar{p}}{dx} + \frac{1}{\bar{T}}\Sigma\bar{h}_i\frac{d\bar{c}_i}{dx} = M_E \tag{4a}$$

where

$$M_E = \frac{2\pi^j}{\dot{m}\bar{T}}\left(\rho_2 u_2 H_2 \delta_2^j \frac{d\delta_2}{dx} - \rho_2 v_2 H_2 \delta_2^j - \rho_1 u_1 H_1 \delta_1^j \frac{d\delta_1}{dx}\right.$$

$$\left. + \rho_1 v_1 H_1 \delta_1^j + \tau_{H,2}\delta_2^j - \tau_{H,1}\delta_1^j\right) - \frac{M_u}{\bar{T}} - \frac{\bar{H}M_m}{\dot{m}\bar{T}}$$

$$= \frac{2\pi^j}{\dot{m}\bar{T}}\left(\rho_2 u_2 (H_2 - \bar{H})\delta_2^j \frac{d\delta_2}{dx} - \rho_2 v_2 (H_2 - \bar{H})\delta_1^j - \rho_1 u_1\right.$$

$$\left. \times (H_1 - \bar{H})\delta_1^j \frac{d\delta_1}{dx} + \rho_1 v_1 (H_1 - \bar{H})\delta_1^j + \tau_{H,2}\delta_2^j - \tau_{H,1}\delta_1^j\right) - \frac{M_u}{\bar{T}} \tag{4b}$$

The effects of mixing are accounted for by the source terms M_m, M_u, M_{c_i}, and M_E. These terms account for the influence of entrainment of the unmixed fuel and oxidizer into the mixing, reacting, and lasing zone (Fig. 3).

Mixing of the reactants is by laminar diffusion. To determine the diffusion coefficient for specie i mixing with a multicomponent mixture of species j, the binary diffusion coefficients D_{ij} are first calculated using the Lennard-Jones (12-6) potential model with polynomial curve fits for the collision integrals as a function of temperature. The multicomponent diffusion coefficient, i.e., the gross diffusion rate for specie i into the multicomponent stream, is determined by

$$D_i = \left[\sum_{j\neq i}\frac{x_j}{D_{ij}}\right]^{-1}$$

where the summation is over the j species in the multicomponent stream and x_j is the mole fraction of specie j.

These source terms are added to the right-hand side of the one-dimensional lasing equations.[8] The flow properties of the entrained gases from the unmixed flow regions are varied with distance downstream to reflect the striations in the flow introduced by nozzle boundary layers. Details are reported in Ref. 16.

III. HF and DF Chemical Rate Models

As is well known, HF (and DF) chemical lasers emit radiant energy from vibrationally excited HF (or DF) produced in a chemically reacting medium which is quite complicated. Chemical reactions both generate and destroy vibrationally excited HF or DF on comparable time scales, while various relaxation and energy transfer processes tend to degrade and redistribute the vibrational excitation which is formed initially by chemical reaction. A great deal of experimental and theoretical effort has been expended during recent years with the aim of measuring, calculating, or estimating rate constants for processes important in chemical lasers. This work has been critically reviewed and augmented from time to time by workers at Aerospace Corporation, and these reviews have come to be the standard sources for rate constants for modeling HF and DF chemical lasers.**

The most recently published of such reviews,[19] which appeared in early 1976, focuses on the HF laser and considers DF only as a relaxer of HF. The recommendations contained therein have been since updated by Cohen, and an informal report of the latest recommendations was forwarded to the authors in May 1976. The main differences between the newer set of rate constants and that in Ref. 19 are as follows:

1) The v-dependence of the low-temperature form for the rate of V-T relaxation of HF by itself and by DF is different, and multiquantum transitions are now included.

2) The v-dependence of the V-T relaxation of HF by H is different. In the newer model, single quantum transitions for $v>2$ are 45 times faster than in the older model, but multiquantum transitions are 4.5 times slower. In the older model, the single and multiple quantum transition rate constants were set equal for $v>1$.

3) Multiple quantum transitions in the V-V transfers between HF molecules are allowed in the newer model and are given the same rate constants as the single quantum transitions, which have the same values as the single quantum transitions of the older model. The older model allowed no multiple quantum V-V transfers.

4) The v-dependence of the $H_2(v)$-HF(v') V-V transfers is linear in v' in the older model, but is somewhat faster than v'^2 in the newer model.

The newer model of Cohen for HF was adopted for this work. Since the details of the model may not be generally known, the rate constants are tabulated in Tables 1a and 1b. These rate constants may also be compared with values found in Ref. 15.

As mentioned previously, the most recent reviews and recommendations on rate constants for chemical laser modeling pertain to HF lasers. The most recent review of DF rate constants available for this work was published in Jan. 1974.[20] It was decided to incorporate the latest ideas concerning HF relaxation into the DF model. The resulting rate constants are tabulated in Tables 2a and 2b, since this model, like the HF model, may not be generally available.

Some differences are evident between the quantum number and temperature dependences on the HF and DF self-V-T relaxation rates shown in these tables. The HF self-V-T rate constants are those recommended by Cohen[21]; note that multiquantum transitions are taken to be as probable as single quantum transitions. Indeed, the rate constant for V-T relaxation of a given v-state to a lower state v' depends only on the value of v not on v'. The total probability for destruction of a state v scales roughly as v^2. Cohen has suggested[21] that the same scaling should apply to DF as well. We have, therefore, derived the DF self-V-T rate constants by using the isotope effect to obtain the $v=1\rightarrow 0$ rate constant from that of HF and applying v^2 scaling to obtain the

**It should be noted that a large fraction of the experimental and theoretical effort alluded to in the text has also been carried out at Aerospace Corporation; this and other relevant work is thoroughly referenced in Ref. 19.

Table 1a Reaction rate[a] data for H_2-F_2 systems (1976): reactions involving generalized collision partners

Reaction	M[b]	A	N	E(kcal)	Comments
$F_2 + F \rightarrow F + F$	*/2.4 F_2, 2.4 F	5×10^{13}	0.0	35.1	
$H + H \rightarrow H_2$ (v)	*/2 H	6.2×10^{17}	-0.95	0.0	v = 0, 1, 2, 3
H_2 (v) = H_2 (v-1)	*/4H_2, 4H	2.5×10^{-9}	4.3	0.0	v = 1, 2, 3
H_2 (v) = H_2 (v')	H	2×10^{13}	0.0	2.72	v = 1, 2, 3; 0 ≤ v' < v
HF (v) = H + F	*	1.33×10^{16}	-1.0	$D^0 - E_{vib}$	0 ≤ v ≤ 9
HF (1) = HF (0)	HF, 0.6 DF	3.0×10^{14}	-1.0	0.0	
HF (2) = HF (v)	HF, 0.6 DF	7.5×10^{13}	-1.0	0.0	v = 0, 1
HF (3) = HF (v)	HF, 0.6 DF	6.0×10^{14}	-1.0	0.0	v = 0, 1, 2
HF (4) = HF (v)	HF, 0.6 DF	5.0×10^{14}	-1.0	0.0	0 ≤ v < 4
HF (5) = HF (v)	HF, 0.6 DF	1.8×10^{15}	-1.0	0.0	0 ≤ v < 5
HF (6) = HF (v)	HF, 0.6 DF	2.5×10^{15}	-1.0	0.0	0 ≤ v < 6
HF (v') = HF (v)	HF, 0.6 DF	2.0×10^{15}	-1.0	0.0	0 ≤ v < v', v' = 7, 8
HF (v) = H (v-1)	HF, DF	3.5×10^{14}	2.26	0.0	0 < v ≤ 8, High Temperature Form.
HF (1) = HF (0)	H	4.5×10^{11}	0.0	0.7	
HF (2) = HF (1)	H	1.6×10^{12}	0.0	0.7	
HF (v) = HF (v-1)	H	2.0×10^{14}	0.0	0.7	3 ≤ v ≤ 8
HF (v) = HF (v')	H	1.0×10^{12}	0.0	0.7	3 ≤ v ≤ 8, v' < v-1
HF (v) = HF (v-1)	Ar, F_2, 2He, N_2	7.7×10^{-7}	5.0	0.0	0 < v ≤ 8
HF (v) = HF (v-1)	3.33 H_2, 17 CF_4	6.0×10^{-7}	1.0	0.0	0 < v ≤ 8
HF (v) = HF (v-1)	F	1.6×10^{13}	0.0	2.7	0 < v ≤ 8
N_2 (1) = N_2 (0)	DF, HF	2.3×10^{1}	3.3	0.7	
N_2 (1) = N_2 (0)	*/0DF, 0HF	1.2×10^{5}	0.0	12.3	

[a] The reaction rate constants are expressed in the form $k = AT^N \exp(-E/RT)$. Units are cm^3-mol^{-1}-s^{-1}. [b] The symbol * means all species act as third bodies with unit efficiency. The symbol */r R, sS means that all species act as third bodies with unit efficiency except R and S, which act with efficiencies r and s, respectively. The symbol rR, sS,... means that the rate so labeled is only for species, R, S,...acting as third bodies with efficiencies r, s,..., respectively.

Table 1b. Exchange and pumping reaction rate[a] data for H_2-F_2 systems (1976)

Reaction	A	N	E (kcal)	Comments
$F + H_2 \rightarrow HF$ (v) + H	$k \times 10^{13}$	0.0	1.60	k = 2.7, 8.8, 4.5 for v = 1, 2, 3
H + HF (v) = H_2 (0) + F	$k \times 10^{12}$	0.0	0.50	k = 3.7, 3.6, 4.2 for v = 4, 5, 6
H + HF (v) = H_2 (1) + F	$k \times 10^{12}$	0.0	0.50	k = 3.7, 7.0, 4.2 for v = 4, 5, 6
H + HF (6) = H_2 (2) + F	10.6×10^{12}	0.0	0.50	
$H + F_2 \rightarrow HF$ (v) + F	$k \times 10^{13}$	0.0	2.4	k = 0.96, 1.6, 4.1, 4.4 for v = 3, 4, 5, 6
HF(v) + HF(v') = HF (v-1) + HF (v'+1)	3.0×10^{15}	-1.0	0.0	1 ≤ v, v' ≤ 8
H_2 (v) + HF (v') = H_2 (v-1) + HF (v'+1)	$k \times 10^{12}$	0.0	0.0	v = 1, 2, 3; k = 0.83, 2.7, 8.3, 19., 38., 75. for v' = 0, 1, 2, 3, 4, 5
N_2 + HF (v) = N_2(1) + HF (v-1)	4.1×10^{12}	-1.0	0.0	1 ≤ v ≤ 9, Low Temperature Form
	3.2×10^{4}	2.0	0.0	1 ≤ v ≤ 9, High Temperature Form

[a] The reaction rate constants are expressed in the form $k = AT^N \exp(-E/RT)$. Units are cm^3-mol^{-1}-s^{-1}.

remaining rate constants. Each state v, decaying with relative probability v^2, has v possible lower states to which to decay. We assume, following Cohen and in the absence of compelling evidence to the contrary, that these should be weighted equally. The resulting array of constants can therefore be expressed in the linear v-scaling form shown. The other chemistry of importance to the D_2-F_2 system is assumed to be identical to that in the most recent review of Cohen[20] on the subject.

Note that individual vibrational levels are treated as separate chemical species, and v is allowed to run from 0 to 9 for both HF and DF. The present form of the BLAZE-II code treats the rotational levels as being always in equilibrium at the translational temperature. Therefore, no dependence of rate constants upon rotational quantum number is included in the present model.

The effects of rotational nonequilibrium in chemical laser oscillators have been studied recently by Sentman[22,23] and Hall.[24] Sentman employs a simplified chemical model in which only two vibrational levels of the lasing molecule are considered, and generalized pumping and relaxation reactions are used, while Hall's model includes five vibrational levels of DF (v=0-4) and a more detailed treatment of pumping and relaxation. Both authors find a tendency for lasing simultaneously on several lines in a vibrational band in the absence of rotational equilibrium. This finding is in harmony with experiment and is in direct contrast to the prediction of lasing on only one line per vibrational band when rotational equilibrium is assumed. Both authors also find that the calculated multiline powers for rotational nonequilibrium are somewhat smaller than the total power over all bands calculated assuming rotational equilibrium; Hall[24] finds the fraction 0.86 for a selected DF case. The ratio of nonequilibrium to equilibrium power is found not to be sensitive to threshold gain or cavity length.[24]

Table 2a Reaction rate[a] data for D_2-F_2 systems (1976); reactions involving generalized collision partners

Reaction	M[b]	A	N	E (kcal)	Comments
$F_2 + F \rightarrow F + F$	*/2.4F_2, 2.4F	5×10^{13}	0.0	35.1	
$D + D \rightarrow D_2$ (v)	*/0D_2, 0D	1×10^{18}	-1.0	0.0	v = 0, 1, 2, 3
$D + D \rightarrow D_2$ (v)	D	3×10^{17}	-0.5	0.0	v = 0, 1, 2, 3
$D + D \rightarrow D_2$ (v)	D_2	1×10^{17}	-0.67	0.0	v = 0, 1, 2, 3
D_2(v) = D_2 (v-1)	*/5D_2, 0D	$1.8 v \times 10^{-3}$	4.3	0.0	v = 1, 2, 3
D_2(v) = D_2 (v')	D	1.6×10^{15}	-0.9	2.4	v = 1, 2, 3 0 ≤ v' < v
DF(v) → D + F	*/5D, 5F, 5DF, 0D_2, 5HF	1.2×10^{15}	-1.0	D^0-E_{vib}	0 ≤ v ≤ 9
DF(v) = DF (v')	DF, 1.58 HF	$1.2 v \times 10^{14}$	-1.0	0.0	1 ≤ v ≤ 9, 0 ≤ v' < v, Low Temperature Form
DF(v) = DF (v-1)	DF, HF	$1.4 v \times 10^{7}$	+2.96	0.0	1 ≤ v ≤ 9, High Temperature Form
DF(v) = DF (v-1)	D_2, 5CF_4	$5.5 v \times 10^{1}$	+3.0	0.0	1 ≤ v ≤ 9
DF(v) = DF (v-1)	F_2, 2He, N_2, Ar	$7.8 v \times 10^{-7}$	+5.0	0.0	1 ≤ v ≤ 9
DF(v) = DF (v-1)	F	$1.6 v \times 10^{13}$	0.0	3.36	1 ≤ v ≤ 9
DF(1) = DF (0)	D	2.4×10^{11}	0.0	1.22	
DF(v) = DF (v-1)	D	6.9×10^{11}	0.0	1.36	v = 2, 3
DF(v) = DF (v-1)	D	8.6×10^{13}	0.0	1.38	4 ≤ v ≤ 9
DF(v) = DF(v')	D	6.9×10^{11}	0.0	1.38	3 ≤ v ≤ 9, 0 ≤ v' ≤ v-2
N_2(1) = N_2(0)	DF, HF	2.3×10^{1}	+3.3	-0.70	
N_2(1) = N_2(0)	*/0DF, 0HF	1.2×10^{5}	0.0	12.3	

[a] The reaction rate constants are expressed in the form $k = AT^N \exp(-E/RT)$. Units are cm^3-mol^{-1}-s^{-1}. [b] The symbol * means all species act as third bodies with unit efficiency. The symbol */r R, sS means that all species act as third bodies with unit efficiency except R and S, which act with efficiencies r and s, respectively. The symbol rR, sS,... means that the rate so labeled is only for species, R, S,...acting as third bodies with efficiencies r, s,..., respectively.

Table 2b Exchange and pumping reaction rate[a] data for D_2-F_2 systems (1976)

Reaction	A	N	E(kcal)	Comments
$F + D_2 \rightarrow DF$(v) + D	$k \times 10^{13}$	0.0	1.97	k = 1.76, 4.0, 6.0, 4.32 for v = 1, 2, 3, 4
D + DF(v) = D_2(v') + F	1.0×10^{13}	0.0	0.5	5 ≤ v ≤ 9, 0 ≤ v' ≤ 3
$D + F_2 \rightarrow DF$(v) + F	$k \times 10^{13}$	0.0	2.46	k = 0.48, 1.02, 1.70, 2.72, 0.82, for v = 5, 6, 7, 8, 9
DF(v) + DF(v') = DF(v-1) + DF(v'+1)	6×10^{15}	-1.0	0.0	1 ≤ v, v' ≤ 8
D_2 (v) + DF(v') = D_2 (v-1) + DF(v'+1)	$k \times 10^{13}$	0.0	0.0	v = 1, 2, 3; k = 0.173, 0.54, 1.2, 2.5, 4.9, 9.7, 19.4, 39.0 for v' = 1, 2, 3, 4, 5, 6, 7, 8
D_2(1) + D_2(v) = D_2(0) + D_2 (v + 1)	$k \times 10^{7}$	1.5	0.0	k = 1.14, 1.64, for v = 1, 2

[a] The reaction rate constants are expressed in the form $k = AT^N \exp(-E/RT)$. Units are cm^3-mol^{-1}-s^{-1}.

Table 3 Breakdown of DF rate model and variations in rate constant magnitudes considered in sensitivity study

Group Name	Typical Reaction	Variations Considered
Pumping Reaction	F + D_2 = DF (v) + D	x 2; x 1/2
Self V-V	DF (v) + DF (v') = DF (v-1) + DF (v+1)	x 4; x 2; x 1/2; x 1/4
DF/D_2 V-V	D_2 (v) + DF (v') = D_2 (v-1) + DF (v' + 1)	All Omitted; All But v = 1 Omitted, $k_{v=1}$ x 1, $k_{v=1}$ x 2, $k_{v=1}$ x 1/2
Self V-T	DF (v) + DF = DF (v') + DF	Δv>1 Omitted, Δv = 1 x 1 Δv>1 Omitted, Δv = 1 x 10
DF/D V-T	DF (v) + D = DF (v') + D	Δv = 1, v = 1, 2, 3, Set Equal to Δv = 1, v>3 Δv>1 Omitted, Δv = 1 x 1 Δv>1 Omitted, Δv = 1 x 2 Δv>1 Omitted, Δv = 1 x 1/2 K = 2×10^{14} T-0.8 exp (-2.2/RT) for all v, v' (1975 Rates)
D_2, CF_4 V-T	DF (v) + D_2 = DF (v-1) + D_2	All Omitted, All x 10
Miscellaneous	F + F + M = F_2 + M D + F + M = DF (v) DF (v) + M = DF (v-1) + M, M = F_2, 2 He, N_2, Ar D + D + M = D_2 (v) + M D_2 (v) + M = D_2 (v-1) + M	All Omitted

Since the conclusions drawn in the present work relate mainly to the dependence of the calculated total power on various parameters, it is felt that the assumption of rotational equilibrium does not materially affect these conclusions.

Since there are a number of uncertainties existing in the rate models for both HF and DF lasers, a study was done in the present work of the sensitivity of the computed laser characteristics to changes in various rate constants. For this purpose, the rate constants were organized into various groups and given changes were made on the group as a whole. The DF model was selected for this study and all calculations were done for one selected test case, the HB5-1989 run of Costello.[25]

The grouping adopted and the rate constant variations considered are detailed in Table 3. It should be emphasized that all variations shown were performed individually with respect to the model of Tables 2a and 2b as the standard.

Table 4 Laser parameters which must be specified to compute closed cavity power

Parameter(s)	How and/or Where Used and Availability
1. Reaction Rates	1. Compute population distribution, small signal gain, temperature and pressure (or area) of flow field. Reasonably well known for DF and HF cold reaction lasers.
2. Pressure or Area of Active Media in Laser Cavity	2. One of these two parameters are required to close the equation system. In small scale devices, i.e., 2 x 8 inches or less, the pressure field will have considerable variation in smaller dimension (perpendicular to lasing and flow direction). Also pressure variations in lasing direction are significant due to curtain - lasing media interaction. Result is that considerable fraction of flow (≅25%) is affected by three dimensional pressure field. Pressure or area usually taken to vary in main flow direction in most models used to date.
3. Nozzle Exit Conditions: Temperature, Velocity (mach number), Composition	3. These parameters are required as a starting condition in laser performance model. These at best vary only in two dimensions for each nozzle and are most significantly affected by combustor and nozzle heat loss, combustor temperature and the development of the thermal and viscous boundary layer in the nozzle. The combustor temperature field is required to compute the nozzle exit boundary layer field. F-atom recombination at the nozzle surface is generally the only physical mechanism which can change the composition as the flow accelerates through the nozzle since residence times are relatively short. Reliable methods are available for computation of the boundary layer development. Surface recombination is poorly understood although some models (30) exist from which to estimate its importance. Availability of these parameters is good but biggest question is the reliability of parameters used in their computation, i.e., *nozzle inlet conditions*, coolant rates or wall temperature of nozzles.
4. Combustor Exit/Nozzle Inlet Conditions	4. Used to compute nozzle exit flow profiles (see 3 above). Heat loss of combustor is required which in turn requires information about the film cooling coefficients. These have become available in recent technology programs. In small device, edge effects can become important and account for relatively large fractional loss in available F-atom due to thermal boundary layer influence.
5. Mirror Reflectivity	5. Used to compute threshold gain. Generally well know at least at the start of test series. May be degraded significantly during testing. Also the minor reflectivity is not the only loss mechanism *present in a closed cavity, although it is the only parameter in which "optical" losses may be* accounted for, e.g., misalignment, diffraction, recirculation of deactivated media in the optical cavity.
6. Mixing Rates and/or Effective Diffusion Coefficients	6. For laminar flows the mixing rate may be computed as accurately as the temperature, T, and pressure, p, fields, since the diffusion coefficients vary according to the relation $D \propto T^{1.5}/p$. The pressure and temperature are determined by the rate of heat release as well as those factors discussed in items 2 and 3 above, whereas for turbulent flows the modeler is faced with selecting the initial turbulence levels or diffusion rates. If the turbulent contribution to the effective diffusion rate becomes important, this assumption reduces the theory to a data fit controlled by the modeler. Model has utility in studying trends but its ability to project a reliable absolute power level is lost.

Table 5 Review of assumptions often used in closed cavity laser performance models

Assumption	Simplification and Consequence
1. Nozzle Exit Profiles are representable by average properties.	1. Leads to one dimensionalization of equations. Theoretical power can be overestimated by as much as 300%.
2. Edge Effects are negligible.	2. Required to "two dimensionalize" the flow field. Implicitly contained in assumption (1) above. In small scale device combustor thermal boundary layer can account for 25% of flow. Similar fractions of flow may be influenced by cavity edge influences.
3. Plane Parallel Mirrors Simulate Optical Cavity.	3. Fabry-Perot Model uncouples flow field calculation from optics wave propogation analysis. Reasonable assumption in multi-mode stable resonator used in closed cavity experiments. However, spill losses are not accounted for in model.
4. Schedule Mixing Rate	4. Severe assumption which allows the modeler to control the rate at which F and D_2 (H_2) are made available for reaction. Reduces the analysis to a "data fit" when attempting to reproduce a specific experiment. However, the model using this assumption does have utility in studying trends.
5. Rotational Equilibrium	5. Greatly reduces the number of dependent variables to be considered. Consequence not too severe in closed cavity simulation but results in prediction of wrong lasing lines and an estimated 30% overly optimistic power prediction. Removal of this assumption essential to the prediction of the correct lasing lines in outcoupled device.
6. Initial Turbulence Level Prescribed	6. Lack of data makes it necessary to estimate initial turbulence level in models using equation(s) to compute effective diffusion coefficient. Result is that the modeler indirectly controls the mixing rate. Fortunately it appears that for most c.w. chemical laser applications the lasing will take *place in the laminar flow regime.*
7. Extent of Mixing, i.e., penetration of each stream into the other, defined by laminar similarity relationship reflecting dependence of mixing in nozzle geometries, exit conditions.	7. Removes requirement of computing detailed two or three dimensional mixing calculation to establish mixing length. Considering current uncertainties in estimating effective temperature and pressure; this approach does not appear to be less attractive than the more exact approach.
8. Properties across the mixing and lasing zone are represented by bulk average properties. Unmixed portions of the flow are not included in the average values but considered separately.	8. Allows the lasing flow field to be modeled using a one dimensional equation system. Details of the flow striations are lost. Explicit computation of the rate of entrainent in terms of profile shape and local diffusion coefficients can not be performed. Require either an empirical expansion be used to compute extent of mixing or introducing additional ordinary differential equations.
9. Cavity Shroud Boundary layers have not separated. Downstream properties do not influence performance.	9. Uncouples the boundary layer influence on cavity performance. Consequence can be that performance projections can be unrealistically high if pressure rise is sufficiently large to induce separation and/or change effective pressure distribution in the cavity.

Note: Assumptions 2, 3, 5, 7, 8 are used in BLAZE-II model.

Therefore, synergistic effects that might result from two or more simultaneous variations are not exposed in this work. The effect of the tabulated rate variations are discussed in Sec. VI.

IV. Cavity Entrance Conditions

The initial conditions required to make a BLAZE-II laser performance calculation are the detailed distribution of the velocity, temperature, and specie concentrations at the nozzle exit plane, i.e., the boundary-layer profiles. These conditions are obtained by first making a combustor calculation to establish the nozzle entrance conditions and, second, by performing a laminar boundary-layer calculation using the combustor exit/nozzle entrance conditions. These analyses are made using the CNCDE computer code which computes the combustor exit/nozzle entrance conditions, assuming a chemical equilibrium condition has been reached in the combustor. Combustor and nozzle heat loss effects are included to obtain the average nozzle throat stagnation temperature. The nozzle boundary-layer characterization technique has been described by Driscoll.[26]

V. Comparisons Between Data and Theory

Considerable insight into the shortcomings of a theoretical model and significance of experimental results can be gained by comparing theoretical predictions with experimental results. A number of experiments were modeled using the BLAZE-II model, which is used in tandem with the CNCDE code (Sec. IV) to characterize the flowfield from the combustor through the nozzle and into the laser cavity. The literature is replete with reports of chemical laser performance. However, only a small fraction of these reports are suitable for modeling studies, since only a limited number of studies provide sufficient detail on the experimental conditions to allow a straightforward calculation to be done. The laser parameters, which must be specified in order to carry out calculations, such as those reported here, are listed and described in Table 4.

However, even the most detailed experiments to date leave much information unspecified, particularly where the fluid dynamical aspects of the probelem are concerned. Therefore, it is still necessary to make a number of simplifying assumptions in order to define the model completely and proceed with computation. Table 5 lists a number of the assumptions often made in laser modeling studies and briefly describes the effects each can have on the calculated results. Assumptions not used in the BLAZE-II model are pointed out. In the calculations reported later for comparison with experiment, no adjustable parameters (such as mixing lengths) were used to achieve a "fit" to the data.

Table 6 Comparison between data and theory

No.	Nozzle	Ref.	Fuels	Lasing on	Exp. I.D.	Ω	R_L	ψ_c	P_c	P_{th}/P_{exp}
1	CL-V (1 x 8)[a]	25	$F_2/C_2H_4/He/D_2$	DF	HB5-1983	36.5	5.0	21.6	6.4	1.17
2	CL-V (1 x 8)	25	$F_2/C_2H_4/He/D_2$	DF	HB5-1988	36.2	6.5	21.7	9.2	1.18
3	CL-V (1 x 8)	25	$F_2/C_2H_4/He/D_2$	DF	HB5-2013	35.7	4.8	31.1	9.3	Chem-lum
4	CL-II (½ x 7)	27	$F_2/H_2/He/D_2$	DF	HB6-1385	18.9	10.5	8.4	0.46	1.06
5	CL-II (½ x 7)	27	$F_2/H_2/N_2/D_2$	DF	HB6-1377	19.8	10.1	9.7	0.61	1.02
6	CL-II (½ x 7)	27	$F_2/H_2/N_2/D_2$	DF	HB6-1320	15.8	9.8	6.0	1.02	1.24
7	CL-II (½ x 7)	28	$F_2/D_2/He/H_2$	HF	783	33	19	11	15	1.40
8	CL-II (½ x 7)	28	$F_2/D_2/He/H_2$	HF	800	34	17	19	1.7	1.30
9	CL XIV	29	$D_2/F_2/He/H_2$	HF	3820	35	2.4	11	6.2	1.30
10	CL XIV	29	$C_6F_6/NF_3/He/H_2$	HF	4019	40	2.8	16	3.3	1.21

[a] Numbers in parentheses refer to nozzle height and width in inches.

We present, in this section, calculated results for the experimental cases listed in Table 6. Each of the calculations was performed assuming laminar mixing, mirror reflectivities reported in the cited references, and using a constant area assumption. Examination of the cavity entrance conditions of case 1983 showed a 3:1 mismatch in nozzle exit pressures. The mismatch in pressure will result in a compression of the D_2/He stream and expansion of the F (and other gases) stream. Consequently, the dominant mixing scale H_{ec} will increase in the process. This effect was considered in the modeling by computing the mixed pressure using an approach that differed from that described in Sec. IV. Specifically, an iterative procedure was used, wherein the downstream mixed pressure is guessed and the isentropic compression/expansion calculations are performed to attain the mixed pressure condition. The resulting conditions approximate the physically more complex phenomena, since boundary-layer effects have been neglected. The exit Mach numbers and temperatures of the inviscid flow are adjusted and boundary-layer profiles fit to the new values. The sensitivity of predictions to this type of calculation is discussed in the following section. As noted in Table 6, the predicted power is in reasonable agreement with the experimental results. The

Table 7. Comparison of baseline calculations with experiment for case HB5-1989

Quantity	Experiment	Calculation
Power, P (kW)	6.9	8.1
Specific Power, σ (kJ/lb)	33.9	39.7
Efficiency, η (kJ/gm - F)	0.73	0.74
Cutoff (cm)	4.34	4.41
Temperature at Cut-off (°K)	–	633
Pressure at Cut-off (torr)	10 [a]	44.2
Temperature at 10 cm (°K)	–	582
Pressure at 10 cm (torr)	20 [a]	38.9
Final Mixing Length, Primary (cm)	–	13.0
Final Mixing Length, Secondary (cm)	–	12.5
Wall Pressure at Streamwise Distance of:		
0.64 cm	5.3	
3.43 cm	6.6	
7.24 cm	14.7	
10.4 cm	14.0	

[a] Estimated wall pressure.

remaining CL-V cases shown in Table 5 were modeled neglecting pressure mismatch effects. The sonic injection CL-II was modeled characterizing the sonic injection slits as supersonic nozzles with an exit dimension equal to the sum of the base region and the sonic slit height. Calculations were made to examine the differences that would be produced by considering the pressure mismatch which occurs (even when expanding to fill in the nozzle base region). The differences were small (<3% for the primary nozzle) due to the relative length scale of the CL-II nozzles and the large percentage of the total mass and momentum contained in the primary. Two trip nozzle cases were successfully modeled using a laminar mixing model, which warrants some explanation. Here it is assumed that the trip produces a wrinkling of the flame sheet which results in a reduction in the laminar mixing scale. Calculations were made for five different trip conditions using the same approach used for cases 1-8 in Table 6. It was found that the model underestimated the observed power consistently by 40-60%. A reduction in the nozzle exit dimension of 20% (not changing nozzle exit conditions) brings all points examined into reasonable agreement with the data.

VI. Sensitivity Study

The CL-V case HB5-1989 was chosen for the sensitivity studies presented here. This nozzle geometry was selected, since no assumptions were required as to how sonic injection (CL-II) or tripping the flow (CL-XIV) influenced laser performance. In Table 7, the baseline calculated results are compared with experiments.[25] For the purpose of this discussion, the variations made on the baseline case are divided into two groups, those involving changes in the kinetic model and those involving changes in other aspects of the input. These two groups are discussed in separate sections.

Sensitivity to Reaction Rate Constants

Table 8 lists the various changes made in the kinetic model and displays the effects of these changes on the calculated results in terms of ratios of various quantities to their baseline values, Table 7.

The pumping reaction rates (cold reaction only) were multiplied and divided by two, with the unanticipated result that the power decreased with faster pumping rate. This may be due to a tendency to destroy a greater fraction of the excited DF by self-V-T when it is formed more rapidly.

Changing the rate of the self-V-V rates has the expected effects on the calculated power, since the tendency of these reactions is to take molecules out of $v = 1$, 2,3 and promote half of them to higher states while de-exciting the other half. Corresponding with this, the percentage of total predicted power that comes from the cold reactions is lower for faster V-V rates.

The DF/D_2 V-V reactions are relatively quite important, since omitting them causes a 38% increase in predicted power.

Table 8 DF modeling sensitivity to reaction rate variations using case HB5-1989 as a baseline [a]

No.	Rate Constants Examined and How Varied	At Cutoff $\bar{X}_{c0}$	At Cutoff $\bar{P}$	At Cutoff $\bar{T}$	At Cutoff $\bar{p}$	At 10 cm Downstream $\bar{T}$	At 10 cm Downstream $\bar{p}$	Mixing Lengths $\bar{X}_{m_1}$	Mixing Lengths $\bar{X}_{m_2}$
1a	Pumping Reaction Rates; x 2	0.98	0.87	1.01	1.01	1.00	1.00	1.0	1.0
b	Pumping Reaction Rates; x 1/2	1.02	1.02	0.99	0.99	0.99	0.99	1.0	1.0
2a	DF Self V-V Rates; x 4	0.95	0.91	1.01	1.01	1.01	1.01	1.0	1.0
b	DF Self V-V Rates; x 1/4	1.03	1.04	0.99	0.99	0.99	0.99	1.0	1.0
3a	DF/D_2 (v) V-V Rates; = 0, All v	1.73	1.38	0.92	0.96	1.00	1.00	1.0	1.0
b	= 0, v>1; x 1/2, v = 1	1.18	1.25	0.99	0.98	0.99	0.99	1.0	1.0
c	= 0, v>1; x 1, v = 1	1.03	1.07	1.00	1.00	1.00	1.00	1.0	1.0
d	= 0, v>1; x 2, v = 1	0.97	0.90	1.01	1.02	1.01	1.01	1.0	1.0
4a	DF Self V-T; Δv>1 x 0, Δv = 1 x 1	1.80	1.82	0.87	0.84	0.93	0.93	1.0	1.0
b	DF Self V-T; Δv>1 x 0, Δv = 1 x 10	0.83	0.80	1.02	1.03	1.05	1.05	1.0	1.0
5a	DF(v)/D V-T; Δv = 1 for V = 1, 2, 3 Set = Δv = 1 for v >3; i.e. x 200 or more, see Table 2a	0.80	0.57	1.11	1.15	1.08	1.08	1.0	1.0
b	; Δv>1 x 0, Δv = 1 x 1/2	1.04	1.02	0.99	0.99	0.99	0.99	1.0	1.0
c	; Δv>1 x 0, Δv = 1 x 1	1.03	1.03	0.99	0.99	0.99	1.00	1.0	1.0
d	; Δv>1 x 0, Δv = 1 x 2	1.01	1.04	1.00	1.00	0.99	0.99	1.0	1.0
e	; All Set = Values Used in 1975 Rate Model	0.81	0.77	1.01	1.02	1.03	1.03	1.0	1.0
6a	DF/D_2,CF_4 V-T; All x 0	1.01	1.02	1.00	1.00	1.00	1.00	1.0	1.0
b	; All x 10	0.88	0.85	1.02	1.02	1.02	1.00	1.0	1.0
7a	Miscellaneous; All x 0	1.01	1.01	0.99	0.99	0.97	0.97	1.0	1.0

[a] See Table 7 for baseline values. Nomenclature: barred quantities are non-dimensionalized by their baselined values. X_{c0} = point at which four v levels cut off., i.e., we avoid counting chain reaction lasing when only a very small fraction of the power is contained therein; P = power; T = temperature; p = static pressure; X_{m1}, X_{m2} = primary and secondary mixing length, final values.

Table 9. DF modeling sensitivity to parameters other than reaction rates [a]

No.	Parameter Examined and How Varied	At Cutoff $\bar{X}_{c0}$	At Cutoff $\bar{P}$	At Cutoff $\bar{T}$	At Cutoff $\bar{p}$	At 10 cm Downstream $\bar{T}$	At 10 cm Downstream $\bar{p}$	Mixing Lengths $\bar{X}_{m_1}$	Mixing Lengths $\bar{X}_{m_2}$
1.	a. Initial Profiles; Slug Average Rather Than Boundary Layer Values, Laminar Mixing.	1.27	1.58	0.87	0.73	1.02	0.91	0.77	>1.6
	b. Same as a. with Scheduled Mixing, 5 cm. Characteristic Length.	1.18	2.50	0.67	0.64	0.83	0.84	0.38	0.40
	c. Same as b. with 0.5 cm to simulate infinitely fast mixing.	0.26	4.28	0.63	0.61	0.82	0.84	0.038	0.040
2.	a. Cavity Pressure; constant = P_3, CALC, 16.8 torr	2.05	1.22	1.00	0.38	1.09	0.38	1.35	>1.6
	b. Cavity Pressure; experimental wall profile used, nozzle exit pressure take equal to pressure at first station.	1.34	2.74	0.87	0.32	1.17	0.51	0.38	0.40
	c. Same as b, but nozzle exit pressure taken equal to calculated P_3.	2.18	1.73	0.97	0.44	1.06	0.51	1.00	1.00
3.	a. Wall temperature = 600°K	1.00	1.00	1.00	0.96	0.98	0.97	0.94	0.88
	b. Wall temperature = 300°K	1.22	1.04	0.99	1.06	1.07	1.12	1.11	1.52
4.	Nozzle Heat Loss; high value simulated with T_1 = 166°K	0.89	0.67	0.90	1.08	0.85	1.03	1.46	1.00
5.	a. F-Atom Recombination; gas phase only, α = 0.8.	0.75	0.85	0.88	0.87	0.93	0.93	1.00	1.00
	b. Same as a, α = 0.5.	0.93	0.77	0.97	0.96	1.06	1.07	1.00	1.00
	c. Wall Only, Fw/Fcore = 0.25.	0.84	0.89	0.98	0.97	0.96	0.95	1.00	1.00
	d. Same as c, Fw/Fcore = 0.50.	0.78	0.86	0.93	0.92	0.92	0.91	1.00	1.00
	e. Same as d, Fw/Fcore = 0.75.	0.80	0.89	0.87	0.85	0.88	0.88	1.00	1.00
	f. Fw/Fcore = 1.00; i.e., no recombination	0.94	0.91	0.82	0.79	0.86	0.86	1.00	1.00
6.	a. Mirror Reflectivities; Ro = RL = 0.99	1.10	1.31	0.97	0.97	0.98	0.98	1.00	1.00
	b. Same as a, Ro = RL = 0.95.	0.88	0.69	1.01	1.02	1.01	1.01	1.00	1.00

[a] See Table 7 for baseline values. Nomenclature: barred quantities are non-dimensionalized by their baselined values. X_{c0} = point at which four v levels cut off., i.e., we avoid counting chain reaction lasing when only a very small fraction of the power is contained therein; P = power; T = temperature; p = static pressure; X_{m1}, X_{m2} = primary and secondary mixing length, final values.

It is observed that D_2 acts as a sink for vibrational energy from the lower DF states. In addition, the D_2 thus excited reacting with F can then lead to formation of DF in states higher than 4. This is manifested in a prediction that only 89% of the power comes from the cold reaction states if the DF/D_2(1) rate is doubled (case 3d, Table 8).

DF self-V-T is quite rapid and destructive of performance in the standard model. Further, multiquantum transitions are very important; omitting these nearly doubles the predicted power. This can be more than compensated by multiplying the single quantum rates by 10. These results suggest that an acceptable, simpler kinetic model might be devised by omitting the multiquantum reactions and increasing the single quantum reactions by a suitable amount.

The processes of deactivation of DF by D atoms are very important in the laser, owing to the rapid formation of D atoms by the cold reaction, but the rates are relatively poorly known. The most influential of these are the rates for single quantum deactivation of $v = 1$, 2, 3. These are significantly slower than the single quantum rates for states higher than 3

in the present model; this leads to rapid dumping of high v molecules into the low v states. This phenomenon would help explain why chain lasers have had only limited success to date. If the low v single quantum rates are allowed to be as fast as those for high v, a drastic reduction in power occurs (case 5a, Table 8). Omitting the multiquantum transitions and changing all the single quantum rates together has little effect on performance. The DF/D V-T rates in common use, up until recently, have a different quantum number dependence than those presently in use. Substituting these 1975 rates decreased power by 25%. It seems clear from these results that better determination of the DF/D V-T rate constants would be of great help for laser theorists.

The relaxation of DF by D_2 and CF_4 is sufficiently slow that omitting these processes from the model hardly affects the predicted power. If they were ten times as fast, however, performance would suffer. Similarly the so-called miscellaneous reactions have little effect on predicted performance and could be omitted by those wishing to use a simplified kinetic model.

Note that none of the rate changes considered have any large effect on temperature or pressure at 10 cm downstream; the mixing distances are unaffected as well.

Sensitivity to Other Variables

Case 1a, Table 9 was selected to study the effect of neglecting nozzle boundary-layer profiles. The BLAZE-II code provides the capability of either computing the mixing length from a laminar flow model or setting that length by designating the extent of the mixing boundary, i.e., at the distance downstream where $\delta_i = H_i$ (Fig. 2). Therefore, cases 1b and 1c were selected to demonstrate the sensitivity of predicted power to mixing length.

We first note that neglecting boundary-layer influences, the predicted power is 58% greater than the baseline calculation. The primary reason for this result is that the temperature of the mixed flow is considerably lower ($\sim 200°K$) than is actually present, due to the boundary layer. Case 1b also shows predicted power levels above the baseline value by factors of 2.5 when a scheduled mixing model is employed to "computationally" reduce the mixing length of the primary stream from 12.5 to 5.0 cm. Finally, case 1c approximates the premixed case by completing the mixing in the first 0.5 cm. The computed power for case 1c is 4.28 times greater than the baseline value, which emphasizes why nozzle designs operating in this flow regime seek to improve the mixing rate, e.g., trip nozzles.[29]

The baseline calculation was run assuming the flow is confined to a constant area. This causes the pressure to rise from the nozzle exit value of 16.8 Torr to 44.2 Torr at cut-off. Cases 2a, 2b, and 2c were selected to demonstrate the effects of other possible cavity pressure profiles. Assumption of constant pressure, case 1a, causes a marked stretching of the lasing zone and a modest increase in power. Using the reported measured wall pressures, however, yields powers higher by factors 2.74 and 1.73, and causes marked shortening of the lasing zone. This is because the measured pressures are much lower than the calculated cavity inlet pressure (see Table 7). Hence, the lower pressure produces a faster laminar mixing rate. Evidently, the expansion fan produces wall pressures which are not characteristic of the bulk of the flow, but much lower.

Nozzle wall temperatures are seldom well-defined in laser experiments. Cases 3a and 3b were selected to show the sensitivity of computed results to this parameter. It is seen that the effect on power is small, but the lasing zone is predicted to be significantly lenghtened when cold walls are employed.

Nozzle heat loss, studied in case 4, can have a large effect on power, perhaps by causing such large delays in the chemistry that DF does not build up to as high concentrations. This would correspond to a more drastic alteration of the pumping reaction rate than was made for case 1b of the kinetics study.

Cases 5a-f treat the effects of F-atom recombination, both in the gas phase and at the nozzle wall.[30] In cases 5a and 5b, gas phase recombination is simulated and the power is reduced markedly. However, no significant hot reaction lasing is predicted, despite having large F_2 concentrations. The cold reaction power loss is due only to lack of F atoms.

The baseline calculation is made under the assumption of complete recombination of F atoms at the nozzle wall. That is, the F-atom concentration is set equal to zero at the wall, and the profile of the F-atom concentration from the wall to the stream centerline is given the typical boundary-layer form. The ratio F_w/F_c, given in Table 9, is the ratio of the F-atom concentration at the wall to that at the nozzle centerline. $F_w/F_c = 1$ implies no recombination of atoms at the wall. In the cases studied, the power was not strongly dependent upon the value taken for F_w/F_c, although all values other than zero yielded lower power. The observation that the power reaches a minimum at an intermediate value of F_w/F_c is surprising and is not yet understood. The fraction of the calculated power in the cold reactions varied from 0.95 for $F_w/F_c = 0$ to 1.0 for $F_w/F_c = 0.75$ and 1.0.

Variation of the mirror reflectivities, cases 6a and 6b had the expected effects on power. This effect is simply a manifestation of the larger amount of excited DF needed to maintain threshold at higher assumed losses. The results show that if internal cavity losses can be held to 1% or less, then about two-thirds of the closed cavity power should be available at 10% out-coupling.

VII. Summary

The BLAZE-II computer code for calculating chemical laser performance has been briefly described, and the procedure used for determining cavity inlet flow conditions for input to BLAZE has been indicated. The kinetic models used to describe the cavity chemistry for HF and DF lasers are presented and compared. The ability of the BLAZE-II computational scheme to model experimental laser performance is demonstrated by comparison of calculated to observed performance for ten recent laser tests.

The results of an extensive study of the sensitivity of the calculated performance to boundary-layer profiles, mixing rates and mechanisms, cavity pressure distribution, wall temperatures, nozzle heat loss, F-atom recombination, mirror reflectivities, and kinetic rate constants are presented and discussed.

Boundary-layer profiles, mixing rates, cavity pressure field, nozzle heat loss, and DF V-T relaxation by itself and by D atoms are identified as particularly critical parameters to which the calculated results are extremely sensitive.

References

[1] Mirels, H. and Spencer, D. J., "Power and Efficiency of a Continuous HF Chemical Laser," *IEEE Journal of Quantum Electronics*, Vol. QE-7, Nov. 1971, pp. 501-507.

[2] Mirels, H., "Interaction Between Unstable Optical Resonator and CW Chemical Laser," *AIAA Journal*, Vol. 13, June 1975, pp. 785-791.

[3] Mirels, H., "Simplified Model of a CW Diffusion Type Chemical Laser—An Extension," Aerospace Rept. TR-0076(6940)-3; *AIAA Journal*, Vol. 14, July 1976, pp. 930-939.

[4] Broadwell, J. E., "Effect of Mixing Rate on HF Chemical Laser Performance," *Applied Optics*, Vol. 13, April 1974, pp. 962-967.

[5] Emanuel, G., Cohen, N., and Jacobs, T. A., "Theoretical Performance of an HF Chemical CW Laser," *Journal of Quantitative Spectroscopy and Radiative Transfer*, Vol. 13, 1975, pp. 1365-1393.

[6] Skifstad, J. G., "Theory of an HF Chemical Laser," *Combustion Science and Technology*, Vol. 6, 1973, pp. 287-306.

[7] Emanuel, G., Adams, W. D., and Turner, E. B., "RESALE-1:A Chemical Laser Computer Program," Aerospace Rept. TR-0172(2776)-1 and Air Force Rept. SAMSO-TR-72-39, March 1972.

[8]Adams, W. D., Turner, E. B., Holt, J. F., Sutton, D. G., and Mirels, H., "The RESALE Chemical Laser Computer Program," Aerospace Rept. TR-0075(5530)-5 and Air Force Rept. SAMSO-TR-75-60, Feb. 1975.

[9]Herbelin, J. M., "A Temperature-Dependent Analytical Diffusion Model for Continuous-Wave ($F+H_2$) Chemical Lasers," presented at the Tri-Service Chemical Laser Symposium, Kirtland AFB, N. Mex., Feb. 1975.

[10]Bullock, D. L., "Unstable Resonators for Chemical Lasers," AFWL-TR-74-201, July 1975.

[11]McDanal, A. J., Ratliff, A. W., and Pearsen, M. L., "LAMP User's Information," Lockheed Rept. R.K.-CR-75-31, Vol. II, June 1975.

[12]Tripodi, R., Coulter, L. J., Bronfin, B. R., and Cohen, L. S., "A Coupled Two-Dimensional Computer Analysis of CW Chemical Mixing Lasers," *AIAA Journal*, Vol. 13, June 1975, pp. 776-784.

[13]Rivard, W. C., Farmer, O. A., and Butler, T. D., "RICE: A Computer Program for Multi-Component Chemically Reactive Flows at all Speeds," Los Alamos Scientific Lab. Rept. LA-5812, March 1975.

[14]Ramshaw, J. D., Mjolsness, R. C., and Farmer, O. A., "Numerical Method for Two-Dimensional Steady-State Chemical Laser Calculations," *Journal of Quantative Spectroscopy and Radiative Transfer*, Vol. 17, 1977, pp. 149-164.

[15]Gross, R. W. F. and Bott, J. F., *Handbook of Chemical Lasers*, John Wiley & Sons, N.Y., ISBN-0-47-32804-9, 1976.

[16]Sentman, L. H., Subbiah, M., and Zelazny, S. W., "BLAZE-II: A Chemical Laser Simulation Computer Program," Tech. Rept. H-CR-77-8, High Energy Laser Lab. Res. and Dev. Command, Redstone Arsenal, Ala., Feb. 1977.

[17]Zelazny, S. W., Driscoll, R. J., Raymonda, J. W., Blauer, J., and Solomon, W. C., "Modeling of DF/HF CW Lasers: An Examination of Key Assumptions," AIAA Paper 77-63, Los Angeles, Calif., Jan. 1977.

[18]Kepler, C. E., Sadowski, T. J., Roback, R., Meinzer, R. A., and Bronfin, B. R., "Demonstration of HF Chain Reaction Laser," Tech. Rept. RK-CR-75-4, U.S. Army Missile Command, Redstone Arsenal, Ala., July 1974.

[19]Cohen, N. and Bott, J. F., "A Review of Rate Coefficients in the H_2-F_2 Chemical Laser System," Aerospace Rept. TR-0076(6603)-2 and Air Force Rept. SAMSO-TR-76-82, April 1976.

[20]Cohen, N., "A Brief Review of Rate Coefficients for Reactions in the D_2-F_2 Chemical System," Air Force Rept. SAMSO-TR-74-14, Jan. 1974.

[21]Cohen, N., private communications, June and Dec. 1976.

[22]Sentman, L. H., "Rotational Nonequilibrium in CW Chemical Lasers," *Journal of Chemical Physics*, Vol. 62, May 1975, pp. 3523-3537.

[23]Sentman, L. H., "Line Suppression and Single Line Performance of a CW HF Chemical Laser," *Applied Optics*, Vol. 15, March 1976, pp. 744-747.

[24]Hall, R. J., "Rotational Nonequilibrium and Line-Selected Operation in CW DF Chemical Lasers," *IEEE Journal of Quantum Electronics*, Vol. QE-12, Aug. 1976, pp. 453-462.

[25]Costello, M. J., "CL-V Test Data," Air Force Weapons Lab. Memo., Kirtland AFB, N. Mex., June 1975. Memorandum supplied to industrial and academic community giving detailed chemical laser data which could be used to compare various computer models on a common basis.

[26]Driscoll, R. J., "A Study of the Boundary Layers in Chemical Laser Nozzles," *AIAA Journal*, Vol. 14, Nov. 1976, p. 1571.

[27]Waypa, J., Reiner, R. J., Bell, S. G., Evans, D. B., and Sugimura, T., "Laser Development for a Chemical Pump," TRW Rept. RH-CR-76-11, May 1976.

[28]Hook, D. L., Hobbs, C. W., Ackerman, R. A., Jarvis, S. J., and Hosack, G. A., "HF/DF Chemical Laser Technology Studies," AFWL-TR-74-150, Kirtland AFB, N. Mex., Oct. 1974.

[29]TRW contract status review for MICOM nozzle technology programs DAAH01-75-C-1000 and DAAH01-75-C-1035, April 1976.

[30]Jumper, E. J., "A Model for Fluorine Recombination at a Metal Surface," Ph.D. Dissertation, Air Force Institute of Technology, Dec. 1975.